

Photon-density waves in macroscopic and microscopic plane-parallel scattering samples

P. J. Peverly, R. E. Wagner, G. H. Rutherford, M. Marsalli,* Q. Su, and R. Grobe

Intense Laser Physics Theory Unit and Department of Physics, Illinois State University, Normal, Illinois 61790-4560

(Received 12 March 2001; published 1 March 2002)

We investigate the validity of the Boltzmann equation to predict the reflection and transmission coefficients for an intensity modulated laser beam passing through a microscopic medium consisting of discrete scatterers. For a one-dimensional model system we demonstrate that the Boltzmann equation works remarkably well for small modulation frequencies, even to describe a medium comprised of only 10 scatterers. Discrepancies can be found only if the modulation wavelength of the laser intensity is commensurate with the spacing between the scatterers and if the medium is sufficiently ordered.

DOI: 10.1103/PhysRevE.65.031908

PACS number(s): 87.90.+y, 05.60.-k, 42.62.Be

I. INTRODUCTION

The Boltzmann equation is regarded as one of the most fundamental descriptions in the science of particle transport in highly scattering or collisional media [1]. It has found applications in areas such as meteorology, oceanography, astrophysics, statistical thermal physics, and medical optics. In astrophysics or neutron physics the Boltzmann equation models the average motion of real particles such as neutrons or atoms [2,3]. In medical optics on the other hand, the Boltzmann equation models the propagation of electromagnetic radiation through highly scattering biological materials [4]. In the latter case this approach is useful only if the physics of the carrier frequency is not so important, so that the radiation field can be characterized by its intensity only. Until few years ago, it was thought that typical wave phenomena, such as diffraction, interference or refraction of electromagnetic waves, could not be described by the probabilistic Boltzmann theory, in which light is modeled by ballistic quasiparticles (“photons”).

About ten years ago [5], it was shown for the first time that if the intensity of a laser field is modulated periodically, a new wave form called a “photon-density wave” [6,7] can be generated inside a highly scattering medium. The coherence of these intensity modulated waves decays on length scales that can exceed the coherence length associated with the carrier frequency by several orders of magnitude [8]. In fact these waves were experimentally shown to exhibit the usual wave properties including interference [9,10], refraction [11,12], diffraction [13], and have shown potential for applications in other areas [14,15].

Most of the theoretical work that followed the experimental breakthroughs made thus far in these investigations was based on analytical solutions in the diffusion limit of the Boltzmann equation. However, for sufficiently high modulation frequencies, experiments have indicated the breakdown of the diffusion approximation, and one has to study the full solution of the Boltzmann equation. Fully analytical forms of the solution prove to be extremely difficult to obtain. Even numerical simulations of the full Boltzmann theory are at the

forefront of computational physics, and numerical solutions to the Maxwell equations in all three dimensions are very difficult [16,17]. In a recent work [18], we have employed a simple one-dimensional model system [19,20] to investigate the breakdown of the diffusion approximation for large modulation frequencies.

In this study we will go one step further and explore the validity of the Boltzmann theory for modulation frequencies whose corresponding wavelength is so short that it is comparable to the average spacing between the individual scattering sites. The Boltzmann equation models the collection of many individual scatterers by considering a very limited number of the medium’s average properties. Only four parameters characterize a scattering medium: the effective index of refraction that determines the propagation speed c in the absence of the scattering, the scattering coefficient μ_s (inverse of the scattering length), the absorption coefficient μ_a , and the scattering phase function $p(\mathbf{\Omega}, \mathbf{\Omega}')$. This function is the probability that an incoming particle associated with solid angle $\mathbf{\Omega}'$ is scattered into direction $\mathbf{\Omega}$. In the following we assume the carrier wavelength of the laser field to be several orders of magnitude smaller than the typical interscatterer spacing.

We intend to address the following questions: How good is a macroscopic Boltzmann theory with respect to modeling a medium that consists of only, say, 100 scatterers? If the wavelength of the modulation of the incoming laser beam becomes comparable to the average spacing between the scattering sites, can the discreteness of the scatterers lead to different collective responses of the medium than that described by the Boltzmann theory? This question is important to the understanding of the rather counterintuitive nonvanishing transmission and zero reflection probability for a medium of finite length in the large-frequency limit predicted by the Boltzmann equation [18,21]. Can one actually use properly chosen modulation wavelengths to excite collective resonances if the wavelength matches the average spacing between the scatterers? The last question is intriguing in a biological tissue, e.g., where the modulation wavelength can be tuned to the average size of the microscopic scatterers (region of different indices of refraction) as well as their spacings.

In order to provide some insight into these questions we have used a simple one-dimensional (1D) model system.

*Present address: Department of Mathematics, Illinois State University, Normal, IL 61790-4520.

This spatially restricted model system has two major advantages: it contains most of the relevant aspects of a 3D system, the full Boltzmann equation can be solved analytically, and the required Monte Carlo simulations can be performed numerically quite efficiently with sufficient accuracy. Additionally, this reduced dimensional model system can also be realized experimentally in optical fibers or other plane-parallel geometries as discussed in Refs. [1], [18], and [19].

The present work is organized as follows. In Sec. II we discuss the Boltzmann equation and its analytical solution. In Sec. III we describe the random-walk computations simulating the propagation of the photon-density waves through a truly heterogeneous medium made up of individual scatterers. In the fourth section we will compare the results obtained from both methods and assess the range of applicability of the Boltzmann theory. We complete this work with a summary and a conclusion.

II. ANALYTICAL SOLUTION OF THE ONE-DIMENSIONAL BOLTZMANN EQUATION FOR THE MACROSCOPIC MEDIUM

The three-dimensional Boltzmann equation (radiative transfer equation) [1] is given by

$$\left(\frac{1}{c}\frac{\partial}{\partial t} + \mathbf{\Omega} \cdot \nabla\right) I(\mathbf{r}, \mathbf{\Omega}, t) = \mu_s \int d\mathbf{\Omega}' p(\mathbf{\Omega}, \mathbf{\Omega}') I(\mathbf{r}, \mathbf{\Omega}', t) - (\mu_s + \mu_a) I(\mathbf{r}, \mathbf{\Omega}, t), \quad (2.1)$$

where $I(\mathbf{r}, \mathbf{\Omega}, t)$ represents the local radiation density propagating in the $\mathbf{\Omega}$ direction, and the inverse of the scattering coefficients μ_s and μ_a describe the effective scattering and absorption lengths. The parameter c is the speed of light in the medium. The scattering phase function $p(\mathbf{\Omega}, \mathbf{\Omega}')$ describes the conditional probability that a laser field in the $\mathbf{\Omega}'$ solid angle is scattered into the $\mathbf{\Omega}$ direction. For simple media this phase function can be constructed from the average differential cross section of the single scatterer. Below we restrict this scattering phase function to only two directions [18]

$$p(\mathbf{\Omega}, \mathbf{\Omega}') = \frac{1}{4\pi} (1-g) \delta(\cos \vartheta + 1) + \frac{1}{4\pi} (1+g) \times \delta(\cos \vartheta - 1), \quad (2.2)$$

where $-1 \leq g \leq 1$ is an adjustable parameter and where $\cos \vartheta \equiv \mathbf{\Omega} \cdot \mathbf{\Omega}'$. The numerical anisotropy factor g is defined as the average cosine of the scattering angle ϑ , $g \equiv \int d\mathbf{\Omega}' p(\mathbf{\Omega}, \mathbf{\Omega}') \cos \vartheta$. Due to its highly bidirectional character, the backward and forward scattering are over-represented at the expense of the scattering events in other directions that are underrepresented. However, this form simplifies our theoretical analysis significantly.

With this bidirectional phase function, the Boltzmann equation can be expressed as a simple coupled set of two differential equations in space x and time t

$$\left(\frac{1}{c}\frac{\partial}{\partial t} + \Omega \frac{\partial}{\partial x}\right) I(x, \Omega, t) = - \left[\frac{\mu_s}{2} (1-g) + \mu_a \right] I(x, \Omega, t) + \mu_s \frac{1}{2} (1-g) I(x, -\Omega, t), \quad (2.3)$$

where $\Omega = \pm 1$ represents the photon flux along the positive and negative x direction. To simplify our notation we assume from now on that $\mu_a = 0$ and introduce the reduced scattering coefficient μ as $\mu \equiv \mu_s (1-g)/2$.

If we introduce the effective photon density $P(x, t) \equiv I(x, +, t) + I(x, -, t)$ and an effective current density $J(x, t) \equiv I(x, +, t) - I(x, -, t)$, we find the following equation for the two-component vector $\mathbf{B} \equiv (P, J)$ in Fourier space defined by

$$P(x) = \int_{-\infty}^{\infty} dt e^{i\omega t} P(x, t),$$

$$J(x) = \int_{-\infty}^{\infty} dt e^{i\omega t} J(x, t), \quad (2x)$$

$$\frac{\partial}{\partial x} \mathbf{B}(x, \omega) = [i(\omega/c) \boldsymbol{\sigma} - 2\mu \mathbf{N}] \mathbf{B}(x, \omega), \quad (2.4)$$

where $\boldsymbol{\sigma}$ denotes the 2×2 matrix $\boldsymbol{\sigma} \equiv \{(0,1), (1,0)\}$ and $\mathbf{N} \equiv \{(0,1), (0,0)\}$ is the nilpotent matrix for which only the last element in the upper row is nonzero.

We assume that the medium extends from $0 < x < W$ and that the index of refraction is the same inside and outside the medium. We can control the incoming photon flux at the left interface of the medium and also the left going wave at the right edge of the medium

$$I(x=0, +, t) = 1 + \cos(\omega t),$$

$$I(x=W, -, t) = 0, \quad (2.5)$$

where $I(x=0, +, t)$ represents the incoming laser field, whose intensity is modulated with frequency ω . Please note that ω should not be confused with the (much larger) carrier frequency of the field, which is not included in the Boltzmann description. Because of the linearity of the Boltzmann equation (2.4) we can find the solutions for a general periodic incoming field of the form $I(x=0, +, t) = \exp(i\omega t)$ and then superpose the corresponding complex solutions for the ac ($\omega \neq 0$) and dc ($\omega = 0$) components. After a little bit of algebra that involves diagonalizing and exponentiating the matrix $[i(\omega/c) \boldsymbol{\sigma} - 2\mu \mathbf{N}]$ and matching the boundaries we obtain as the solution inside the medium

$$P(x) = \{C(x)[C(W) - S(W)(i\omega/c - 2\mu)] + S(x)(i\omega/c - 2\mu)[C(W) - S(W)i\omega/c]\} / [C(W) - S(W)] \times (i\omega/c - \mu),$$

$$J(x) = \{S(x)i\omega/c[C(W) - S(W)(i\omega/c - 2\mu)] + C(x) \times [C(W) - S(W)i\omega/c]\} / [C(W) - S(W)] \times (i\omega/c - \mu), \quad (2.6)$$

where we have defined the complex functions $S(x) \equiv \sinh(\kappa x)/\kappa$ with $\kappa \equiv \sqrt{[-2i\omega\mu/c - (\omega/c)^2]}$ and $C(x) \equiv \cosh(\kappa x)$. The eigenvalue κ can be decomposed into its real and imaginary parts according to

$$\kappa = -\left[\frac{\omega}{c}\left(\frac{\omega^2}{4c^2} + \mu^2\right)^{1/2} - \frac{\omega^2}{2c^2}\right]^{1/2} + i\left[\frac{\omega}{c}\left(\frac{\omega^2}{4c^2} + \mu^2\right)^{1/2} + \frac{\omega^2}{2c^2}\right]^{1/2},$$

which indicates an effective wavelength inside the medium that can be much smaller than the wavelength $\lambda = 2\pi c/\omega$ in the absence of any scattering if $\mu > \omega/(2c)$.

The large- and small-frequency limit for Eq. (2.6) can be read off immediately

$$\lim_{\omega \rightarrow 0} P(x) = [1 + 2\mu(W-x)]/[1 + \mu W],$$

$$\lim_{\omega \rightarrow \infty} P(x) = \exp(i\omega x/c)\exp(-\mu x). \quad (2.7)$$

Two observations are in order. First, it is interesting to note that in one spatial dimension the dc component decays linearly as a function of the distance. This component also shows an unexpected dependency on the total length of the medium W . The distance x_{decay} after which $P(x)$ has decayed by a factor of $1/e$ increases linearly with the total length of the medium, $x_{\text{decay}}(\omega=0) = [(e-1)(1+\mu W) + e\mu W]/[2\mu e]$, whereas in the large-frequency limit the ac component decays purely exponentially: $x_{\text{decay}}(\omega \rightarrow \infty) = 1/\mu$. On the other hand, the ratio of the photon probability at the right and left edges of the medium, $1/(1+2\mu W)$, decreases with increasing medium length for $\omega=0$ as expected.

Second, the transmitted intensity does not vanish in the large-frequency limit. One could have (incorrectly) expected that the smaller the wavelength of the intensity modulation, the ‘‘easier’’ it would be for a diffusive medium to attenuate these short wavelength oscillations. But the large-frequency limit approaches a form independent of the frequency. We will investigate if the Boltzmann equation holds for frequencies so large that the modulation wavelength becomes comparable to the average spacing between the scattering sites. In the same limit, the intensity distribution becomes independent of the spatial length of the medium W .

In the limit of an infinitely extended medium ($W=\infty$) we obtain only reflected light

$$\lim_{W \rightarrow \infty} P(x) = \frac{\kappa - 2\mu + i\omega/c}{\kappa - \mu + i\omega/c} e^{\kappa x}. \quad (2.8)$$

Since κ [defined below Eq. (2.6)] has a negative real part, $P(x)$ in Eq. (2.8) decays in space and approaches zero as $x \rightarrow \infty$ as expected.

Using our boundary conditions for $I(x=0,+,t)$ and $I(x=W,-,t)$ we obtain the coefficient for the transmitted portion for the steady state as $T_B(\omega) \equiv P(x=W)$ and $R_B(\omega)$

$\equiv P(x=0) - 1$ for the reflected portion. Using the analytical solution of Eq. (2.6) we obtain

$$R_B(\omega) = S(W)\mu/[C(W) - S(W)(i\omega/c - \mu)],$$

$$T_B(\omega) = [C(W)^2 - i\omega/c S(W)^2(i\omega/c - 2\mu)]/[C(W) - S(W) \times (i\omega/c - \mu)]. \quad (2.9)$$

Note that only for the dc signal do we have the conservation law $R_B(\omega=0) + T_B(\omega=0) = 1$. Below we will compare these Boltzmann coefficients with those obtained from a Monte Carlo simulation for a truly microscopic medium.

III. NUMERICAL SOLUTION FOR MICROSCOPIC MEDIA

Our medium is characterized on a microscopic scale by an array of N point scatterers that are localized at random positions x_n ($n=1,2,\dots,N$) within a spatial strip of total length W . We have chosen the *average* spacing between the scatterers $d \equiv \langle d_n \rangle = \langle x_{n+1} - x_n \rangle = 1$ in all of our simulations. From now on we will measure all lengths such as λ , $1/\mu$, and W in units of d . Our unit system of time is uniquely defined if we also set the speed $c=1$. We change the *degree of order* in this system by varying the standard deviation of the uniform distribution of these spacings Δd between $\Delta d=0$, corresponding to an equidistant arrangement of scatterers as in a perfect crystal, to $\Delta d \approx 0.3d$ to represent a random medium. Because $p(\mathbf{\Omega}, \mathbf{\Omega}')$ is independent of the position, all scatterers are assumed to have the same scattering strength.

Each scatterer is assigned a reflection probability of r . A perfectly transmitting medium would have $r=0$, whereas for $r=1$ any incoming photon is reflected. Because of the one-dimensional nature of our system the anisotropy factor g introduced in Sec. II is directly related to r via $g=1-2r$. In order to relate the microscopic parameters W , N , and r to the macroscopic parameter μ_s , we have to calculate first the total probability of reflection for N scattering sites where each site has a reflection probability of r_i and a transmission probability of $t_i=1-r_i$. For two sites ($N=2$) one can just sum up the probabilities for all paths that scatter once, three times, five times, etc., according to $R_{N=2} = r_1 + t_1 r_2 t_1 + t_1 r_2 r_1 r_2 t_1 + t_1 r_2 r_1 r_2 r_1 r_2 t_1 + \dots = [r_1 + r_2 - 2r_1 r_2]/[1 - r_1 r_2]$. Generalizing this counting scheme for N scatterers of equal reflection probability $r=r_i$ we obtain the total reflectivity,

$$R_N = Nr/[1 + (N-1)r]. \quad (3.1)$$

If we equate this with the reflection probability for $\omega=0$ from the Boltzmann system $R_B(\omega=0) = \mu W/[1 + \mu W]$ from Eq. (2.9) we obtain the following relation between the microscopic and macroscopic parameters $\mu_s = N/[W(1-r)]$. For a sufficiently small reflectivity r the effective scattering length $1/\mu_s$ of the Boltzmann theory is equal to W/N that is the average distance between the scattering sites. This

result is expected. The reduced scattering coefficient $\mu = rN/[W(1-r)]$, however, vanishes for perfect transmission ($r=0$).

We now describe some technical details of the numerical Monte Carlo simulations. We have injected M photons into the medium, each of which has a probability of r to be scattered at each location x_n . In traditional Monte Carlo simulations used for finite laser pulse propagation through biological tissues [22], a photon travels a random time and is then redirected into a new random angle. In these simulations each photon interacts with a different medium, and even a single photon experiences a time-dependent medium whose scattering sites change their location and scattering strength.

In our simulations there are two distinct differences, which make our simulations computationally more demanding. First, we are interested in steady states, which require large interaction times and therefore a larger number of photons M . Second, as we are interested in exploring resonance-like effects, we require the arrangement of the scatterers to be absolutely identical for each photon.

In order to simulate our boundary condition according to $I(x=0,+,t) = 1 + \cos(\omega t)$, we could distribute all of our photons initially to the left of our medium ($x < 0$) with an initial density given by $I(x,+,t=0) = 1 + \cos(\omega x/c)$ for $x < 0$ and $I(x,+,t=0) = 0$ for $x > 0$. This extended probability distribution would then travel to the right, in agreement with our boundary condition $I(x=0,+,t) = 1 + \cos(\omega t)$. A calculation of this type, however, would require us to monitor the time evolution of all spatial locations at all times. In order to reduce the computational time significantly, we could inject the train of (right traveling) photons at a source located at $x = -20$. The ‘‘pump rate’’ at the source is then varied as a function of time with frequency ω . A point source (at $x = -20$), however, would require continuous generation of photons. To avoid the numerical burden associated with the extremely small time steps required to imitate continuous pumping, we create a larger section of the wave train in periodic time intervals associated with an effective spatially extended source ($-20 < x < -19$). The adjoining sections of the wave train are phase matched to mimic the desired continuous periodic wave train. In other words, the spacing between neighboring photons is chosen deterministically such that the resulting photon density is described by $I(x,+,t=0)$. This involves the inversion of a transcendental trigonometric equation, which we have performed using a rapidly converging iteration scheme.

The total photon probability density is then determined by summing up several mini-Gaussians that are centered around the location $x_m(t)$ of each photon at time t ,

$$P(x,t) = N \sum_{m=1}^M \exp[-\{x - x_m(t)\}^2/s^2], \quad (3.2)$$

where the width of each mini-Gaussian was chosen large enough to overlap sufficiently with the Gaussian of its nearest neighbor, but much smaller than the length scale of interest, which is of the order of the wavelength in our problem. N denotes the normalization constant that depends on the pump rate at the source. In practical terms, our simulations

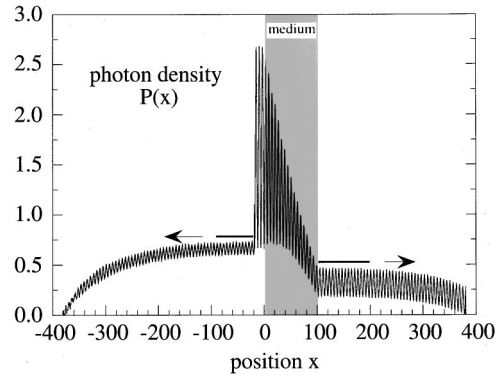


FIG. 1. The final light intensity distribution as a function of position (in units of the average interscatterer distance d). Sketch of the geometry used in the calculation for an index-matched scattering medium. (The parameters used in the simulation were $M = 100\,000\,000$ photons, $\omega = 1.05$, $N = 100$ scatterers, $r = 0.02$, $W = 100$, $\Delta d = 0.287$, $t = 400$, and the width of each mini-Gaussian was $s = 0.01$, the photon source is located at $x = -20$.)

were typically performed with M in the range of 100 million photons, and a width s roughly 100 times smaller than the wavelength. We found these parameters sufficient in all of our simulations to make the error due to the discreteness of the photons negligible.

The parameters that we have used in our simulations are $N = 100$, $W = 100$, and $r = 0.01$ corresponding to $\mu = rN/[W(1-r)] \approx 0.01$. We have chosen these parameters because in this regime the medium has roughly equal amounts of reflected and transmitted fields for the dc component, $R_B(\omega=0) = 0.5025$ and $T_B(\omega=0) = 0.4975$.

In order to test the steady state data obtained from the Monte Carlo simulation, we have also generalized the transfer matrix approach typically used in quantum mechanics [23] in order to describe intensity modulated laser fields. In this approach each point scatterer is represented by a 2×2 matrix linking the input and output channels,

$$\mathbf{M}_n = \begin{pmatrix} 1 - r_n/t_n & r_n/t_n \exp[-i4\pi\omega x_n/c] \\ -r_n/t_n \exp[i4\pi\omega x_n/c] & 1/t_n \end{pmatrix} \quad (3.3)$$

where r_n and t_n are the individual scattering coefficients and x_n is the location of the n th scatterer. The collective properties of the entire medium can be obtained by multiplying the matrices numerically, $\mathbf{M} = \prod_{n=1}^N \mathbf{M}_n$ where the matrix \mathbf{M}_1 (associated with the leftmost located scatterer) should be the right most factor, as the individual matrices do not commute. The total reflection and transmission coefficients can be computed from the product matrix \mathbf{M} via $R = -M_{1,2}/M_{2,2}$ and $T = \det(\mathbf{M})/M_{2,2}$. This approach, however, is not well suited for analyzing the time-dependent aspects of the dynamics.

IV. DISCUSSION OF THE RESULTS

In Fig. 1 we display a typical photon probability $P(x,t)$ of Eq. (3.2) obtained as a histogram over $M = 100$ million photons after an interaction time of $t = 400$. The photon source is

located at $x = -20$. In the absence of the scattering medium we would obtain a distribution $P(x, t) = [1 + \cos(\omega t - \omega x/c)] \theta(x + 20)$, with θ the unit step function. The spatial domain can be divided up into six different regions, ranging from $380 < x < -100$, $-100 < x < -20$, $-20 < x < 0$, $0 < x < 100$, $100 < x < 200$, and $200 < x < 380$. The outermost regions ($-380 < x < -100$ and $200 < x < 380$) correspond to the early time response of the medium to the incoming field. This transient part corresponds to the time it takes for the incoming photons to “fill up” the medium with light in order to establish the steady state inside the medium. The steady state is established when the pump rate (number of photons created at $x = -20$ per time unit) is identical to the sum of the rates of the transmitted and reflected photon fluxes escaping at the two boundaries $x = 0$ and $x = 100$. The steady state is then characterized by transmitted and reflected intensity with constant amplitudes as shown for $-100 < x < -20$ and $100 < x < 200$. Comparing the amplitudes of the steady state we clearly see that the ac component in the transmitted portion has been less attenuated than its counterpart in the reflected intensity. The fact that in both curves the minima are far above zero indicate that the ac component has been attenuated more compared to the dc component.

The photons inside the region $-20 < x < 0$ are the sum of the incoming (right going) and the diffusively reflected light. In this region the dc component of the reflected light prohibits the minima of $P(x)$ from being equal to zero. The very front edge close to $x = 380$ is sometimes called the “ballistic light” as it corresponds to that portion of the very early photons that could pass through the medium without any reflection. The following photons have experienced a few reflections and are called “snake light” [4].

Inside the medium ($0 < x < 100$) it is interesting to note that the maxima and the minima of $P(x)$ decay quite differently as a function of x . Due to the complicated interference of forward and backward scattered light close to the entry surface of the medium at $x = 20$, the amplitude associated with the minima actually grows first to about $x = 20$, whereas for $x > 20$ it decays. We should note that the graph in Fig. 1 was displayed with 24 000 points in order to resolve details on length scales much smaller than the wavelength.

The steady state distribution for the reflected and transmitted photons is of special interest in this work. It is used to determine the reflection and transmission coefficients $R(\omega)$ and $T(\omega)$, which have been obtained using a nonlinear least squares fitting algorithm to determine the phase and the amplitude. These numbers were then compared directly with the analytical reflection and transmission coefficients $R_B(\omega)$ and $T_B(\omega)$ obtained from the Boltzmann theory of Eq. (2.9).

We have compared the two values for the transmission coefficient $T(\omega)$ and $T_B(\omega)$ and computed the relative error $E = ||T_B(\omega) - |T(\omega)|| / |T(\omega)|$ of the Boltzmann theory for various media that differ by degree of randomness as characterized by the standard deviation of the uniformly distributed spacings between the scatterers Δd . The parameter $\Delta d = 0$ corresponds to an equidistant arrangement of scatterers as in a perfect crystal, whereas for $\Delta d \approx 0.29$ the distances between the scatterers are random.

With the exception of a certain specific subset of modu-

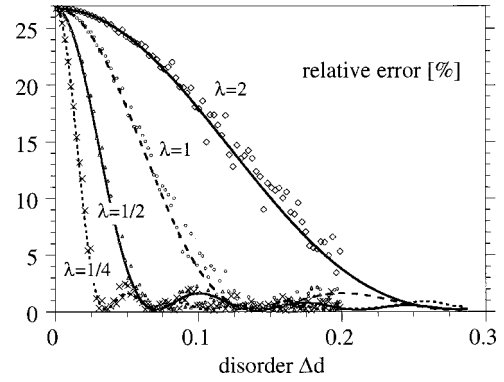


FIG. 2. The error of the Boltzmann theory for a microscopic medium as a function of the degree of order Δd (in units of d) for various wavelengths (in units of d) for the transmission coefficient. The markers are the data from the Monte Carlo simulations with $M = 10\,000\,000$ photons, $N = 100$ scatterers, $r = 0.01$, $W = 100$, $t = 400$ (in units of d/c), and the width of each “mini-Gaussian” was $s = 0.01$, the photon source is located at $x = -20$.

lation frequencies to be discussed below, practically all simulations indicated that the Boltzmann predictions had errors of at most 0.5%, independent of the degree of randomness. This clearly demonstrates that a medium consisting of only $N = 100$ scatterers can be adequately approximated by the macroscopic Boltzmann theory. We should note that the range of frequencies investigated in our studies corresponds to wavelengths much larger than the entire medium ($\lambda = 500$) to those as small as a tenth of the average spacing ($\lambda = 0.1$).

The only situation we encountered where the Boltzmann equation becomes inapplicable is for very special choices of the wavelength ($\lambda = 2/n, n = 1, 2, 3, \dots$) for nearly perfectly ordered media ($\Delta d \approx 0$). These exceptional cases for which the Boltzmann approach fails are displayed in Fig. 2.

The largest failure of the Boltzmann equation occurs for a wavelength that is twice the interscatterer spacing, $\lambda = 2$. In contrast to scattering of electromagnetic radiation at interfaces with different indices of refraction, the intensity wave does not change its phase when scattered. Correspondingly, any light path that is based on two scattering events interferes fully constructively with the nonscattered portion. This is an interesting resonance effect that is reminiscent of Bragg scattering in perfect crystals. However, in contrast to the usual Bragg scattering associated with the carrier frequency of the field, in our case the interference happens on the length scale of the intensity modulation. Similarly constructive paths can also be found for $\lambda = 1, \frac{1}{2}$, and $\frac{1}{4}$, however, the associated resonances are much narrower compared to $\lambda = 2$. For $\lambda = 4$ (not shown) there are constructive as well as destructive paths possible, and the maximum error was less than 0.2%. The data represented by the markers were obtained from the Monte Carlo simulation, whereas the curves are the result of the transfer matrix approach.

To analyze the breakdown of the Boltzmann theory to describe a perfectly ordered media in more detail, we have displayed the error E in Fig. 3 for a larger range of the modulation wavelength $0.1 < \lambda < 2.2$. With the exception of the few frequency cases discussed above, the error due to the

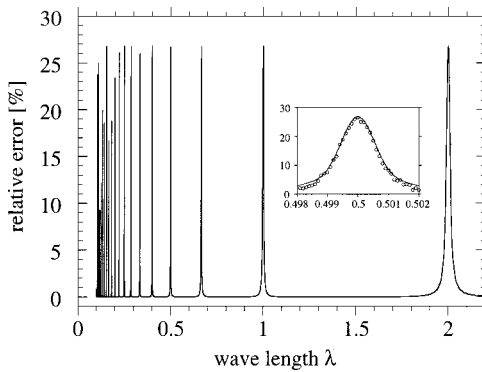


FIG. 3. The error of the Boltzmann theory for a perfectly ordered medium ($\Delta d=0$) as a function of the wavelength λ (in units of d). The inset shows the resonance for $\lambda=0.5$, the continuous line is the prediction from the transfer matrix approach. The circles are the data from the Monte Carlo simulation using $M=10\,000\,000$ photons. (The parameters used in the simulation were $N=100$ scatterers, $r=0.01$, $W=100$, $t=400 d/c$, and the width of each mini-Gaussian was $s=0.01$, the photon source is located at $x=-20$.)

Boltzmann approximation stays below the upper limit of 0.5%. In the inset we have displayed the resonance around $\lambda=0.5$ on a much finer scale. The peak has a half-width of about 0.0014, which is less than 0.3% of the wavelength. In other words, only wavelengths in the extremely narrow range of $0.498 < \lambda < 0.502$ are able to “resonate” with a perfectly ordered medium. In summary, unless that medium is perfectly ordered and the wavelength is a fraction of 2, the Boltzmann theory explains the transmitted portion of the steady state intensity remarkably well.

All previous calculations were performed for the medium with $N=100$ scatterers. Let us now demonstrate the breakdown of the Boltzmann equation for media with a smaller number of scatterers. We have kept the corresponding macroscopic averaged quantities such as μ and W constant and adjusted the individual scattering strength r as we varied N according to $r = \mu W / (\mu W + N)$. We chose the medium with a maximum amount of disorder.

In Fig. 4 we display the transmission and reflection coefficients as functions of the modulation frequency ω for media consisting of $N=5$ and 10 scatterers. The continuous curve

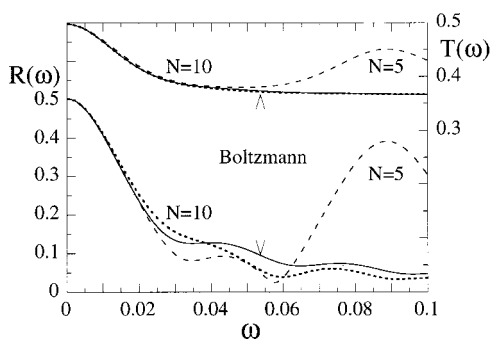


FIG. 4. The transmission and reflection as a function of the modulation frequency of the laser (in units of c/d) for a medium with $N=5$ and $N=10$ scatterers. The continuous line is the prediction of the Boltzmann equation.

corresponds to the prediction of the Boltzmann equation. For small modulation frequencies the agreement with the Boltzmann equation is remarkably good even for very diluted media consisting of only $N=10$ scattering sites. At the same time the optical properties of the $N=5$ medium depends very much on how the individual scatterers are arranged. As the frequencies get larger the Boltzmann equation works slightly better to predict the transmission than the reflection coefficient. For media with more than $N=50$ random scatterers the predictions of the Boltzmann equation are quite reasonable for all frequencies.

V. SUMMARY AND CONCLUSIONS

We have tested the applicability of the Boltzmann scattering theory to describe the optical properties for a system with only a finite number of randomly located scatterers. By equating the total reflection probability for the continuous and the heterogeneous media, we derived a relation between the microscopic reflection coefficient of each slab and macroscopic parameters such as the scattering coefficient μ . The validity of this relation is established for the more general case in which the intensity is modulated as a function of time. With the exception of very specific modulation wavelengths and a sufficient amount of order in the system the Boltzmann theory is surprisingly reliable to describe even heterogeneous media that are comprised of only 10 scatterers. The Boltzmann theory even works remarkably well in a region in which the wavelength associated with the modulated intensity is short enough and comparable to the inter-scatterer spacing thus permitting at least in principle the resolution of the discreteness of the scatterers. One reason why even a medium comprised of only $N=10$ scatterers can be described by a theory that is based on a continuous scattering medium could be the fact that for our parameter regime the average reflected and transmitted photons experience many more than just 10 scattering events.

The main result reported in this work is certainly not the final goal of this line of inquiry. The long term goal of our studies is to find an improved description of the optical properties of highly scattering media that goes even beyond the macroscopic Boltzmann theory. As mentioned in the introduction, the Boltzmann equation cannot describe diffraction, interference or refraction of electromagnetic fields, and it would be quite desirable to find a new theoretical framework that avoids all the probably unnecessary microscopic details of the medium but nevertheless can include some wave aspects of light. So as a first step towards this theory, it is quite important to clearly identify inaccuracies in a continuous medium description that are due to the averaging and those that are intrinsically due to the omission of the coherence and general wave nature of the photons. In a related work [24] we have begun to investigate the importance of the phase of the electromagnetic field for heterogeneous random media by comparing the predictions of the Maxwell equations with that of an intensity theory.

The present analysis has been performed for a one-dimensional random medium that can be realized experimentally by a sample of plane-parallel dielectric layers. The

reader might wonder about the generality of the conclusion for those media that do not have a symmetry permitting a reduced dimensional description. We should point out that even numerical solutions to the three-dimensional Boltzmann equation are presently very difficult—if not impossible—to obtain. However, we would like to remark that there is no fundamental difference in the physics between a single scattering event in a one- or three-dimensional description and we would expect that our conclusion about the applicability of the Boltzmann equation for truly heterogeneous media should also hold in two or three dimensions. In fact one can show that the essential aspects of the scattering theory such as the partial wave decomposition or even the optical theorem [25] have their direct counterpart in two- and even one-dimensional scattering systems. In contrast to the ballistic transport of particles described in this work, the propagation dynamics of a wave, however, could depend

more strongly on the spatial dimensionality for weakly scattering media due to the impact of the polarization. In one- and two-dimensional systems the polarization direction need not change, but in three dimensions this change is unavoidable. Our future work is directed towards these questions.

ACKNOWLEDGMENTS

We would like to thank E. Gratton for triggering our interest in photon-density waves and useful discussions during mutual visits. We also acknowledge discussions with S. Menon. This work has been supported by the NSF. We also acknowledge support from the Research Corporation and BLV. The numerical work has been performed at NCSA. R.E.W. and P.J.P. thank the ISU Undergraduate Honors Program for support.

-
- [1] S. Chandrasekhar, *Radiative Transfer* (University Clarendon Press, Oxford, 1950).
 - [2] For a review, see, e.g., M. C. van Rossum and T. M. Nieuwenhuizen, *Rev. Mod. Phys.* **71**, 313 (1999).
 - [3] A. Ishimaru, *Wave Propagation and Scattering in Random Media* (Academic, New York, 1978), Vols. 1 and 2.
 - [4] B. B. Das, F. Liu, and R. R. Alfano, *Rep. Prog. Phys.* **60**, 227 (1997).
 - [5] E. Gratton, W. Mantulin, M. J. van de Ven, J. Fishkin, M. Maris, and B. Chance, in *The Third International Peace through Mind/Brain Science Conference*, Hamamatus, 1990 (Loats Associates, Westminster, MD, 1990), p. 183.
 - [6] A. Yodh and B. Chance, *Phys. Today* **48**(3), 34 (1995).
 - [7] A. Madelis, *Phys. Today* **53**(8), 29 (1995).
 - [8] For a more detailed account see, J. B. Fishkin, Ph.D. thesis, University of Illinois, 1994.
 - [9] J. M. Schmitt, A. Knuttel, and J. R. Knudsen, *J. Opt. Soc. Am. A* **9**, 1832 (1992).
 - [10] B. Chance, K. Kang, L. He, and J. Weng, in *Int. Soc. Oxygen Transport to Tissue*, edited by P. Baupel (Plenum, New York, 1993).
 - [11] M. A. O'Leary, D. A. Boas, B. Chance, and A. G. Yodh, *Phys. Rev. Lett.* **69**, 2658 (1992).
 - [12] For a more detailed account see, D. A. Boas, Ph.D. thesis, University of Pennsylvania, 1996, available under <http://rabi.nmr.mgh.harvard.edu/DOT/Publications/Dissertation/Boas96/diss.html>
 - [13] J. Fishkin and E. Gratton, *J. Opt. Soc. Am. A* **10**, 127 (1993).
 - [14] For a more detailed account see, M. A. O'Leary, Ph.D. thesis, University of Pennsylvania, 1996, available under http://www.nmr.mgh.harvard.edu/DOT/Publications/Dissertation/Oleary96/oleary_diss.html
 - [15] S. A. Prahl, Ph.D. thesis, University of Texas, 1988, available under <http://omlc.ogi.edu/pubs/pdf/prahl88.pdf>
 - [16] W. Harshwardhan, Q. Su, and R. Grobe, *Phys. Rev. E* **62**, 8705 (2000).
 - [17] A. Tavlove, *Computational Electrodynamics the Finite-Different Time-Domain Method* (Artech House, Norwood, 1995).
 - [18] Q. Su, G. H. Rutherford, W. Harshwardhan, and R. Grobe, *Laser Phys.* **11**, 94 (2001).
 - [19] M. J. C. van Gamert, A. J. Wells, and W. M. Star, in *Optical-Thermal Response of Laser-Irradiated Tissue*, edited by A. J. Wells and M. J. C. van Gamert (Plenum, New York, 1995), Chap. 3.
 - [20] For a review on the spectral properties of 1D random lattices, see, e.g., T. M. Nieuwenhuizen, *Physica A* **125**, 197 (1984); **120**, 468 (1983).
 - [21] J. B. Fishkin, S. Fantini, M. J. vandeVen, and E. Gratton, *Phys. Rev. E* **53**, 2307 (1996).
 - [22] For reviews and Monte Carlo programs, see, e.g., <http://omlc.ogi.edu/software/mc>
 - [23] See, e.g., D. J. Griffiths, *Introduction to Quantum Mechanics* (Prentice-Hall, Englewood Cliffs, NJ, 1994), Chap. 2.
 - [24] S. Menon, Q. Su, and R. Grobe (unpublished).
 - [25] J. H. Eberly, *Am. J. Phys.* **33**, 771 (1965).